ABSOLUTE DATING OF RECENT SEDIMENTS IN THE CYCLONE-INFLUENCED SHELF AREA OFF BANGLADESH: COMPARISON OF GAMMA SPECTROMETRIC (^{137}Cs, ^{210}Pb, ^{228}Ra), RADIOCARBON, AND ^{32}Si AGES

Axel Suckow[1] • Uwe Morgenstern[2] • Herrmann-Rudolf Kudrass[3]

ABSTRACT. A geochronological survey of the Bengal shelf area involved results from more than 20 sediment cores dated using gamma spectrometry and the nuclides ^{137}Cs, ^{228}Ra, ^{226}Ra, and ^{210}Pb. In some cores, which contained older sediments, ^{32}Si and ^{14}C were determined to examine the possibility to extrapolate the obtained chronologies to century and millennial scale. Geochronological work in this region is faced with problems of cyclone-induced sediment reworking, grain-size effects on fallout nuclides, scarcity of carbonates, unknown ^{14}C reservoir effect and sedimentation rates that are too high to obtain sediment cores long enough to establish a chronology. Despite these problems, comparison between the results of the different dating methods provided the most reliable sediment balance to date for the submarine delta of the Ganges-Brahmaputra river system and indicated that on a time scale of several centuries at least 35% of the annual sediment load is deposited.

INTRODUCTION

With an estimated sediment load of 1.7 billion tons (Milliman and Meade 1983) or 1 km^3 annually, the Ganges, Brahmaputra, Meghna river system is one of the largest in the world. About one third of the sediment load is deposited, at least temporarily, on the flood plain of the delta (Allison et al. 1998; Goodbred and Kuehl 1998; 1999). The fate of the remaining two thirds of sediment is not well known.

Where the sediments enter the Indian Ocean, there is a shallow water region (the "inner shelf") with a mean depth of 7 m, extending roughly 300 km along the shore and 60 km offshore (Moore 1997; Figure 1). A volume estimate shows that this area of shallow water should be filled up in less than 150 years. However, there have been few changes along the delta front and coastline during the last 200 years (Allison, 1998). Consequently, the sediments must be in dynamic equilibrium on the inner shelf. Tidal currents that mostly transport sediment westward (Barua et al. 1979) and tropical cyclones that episodically redistribute large amounts of resuspended fine-grained sediment, are the dominant processes of sediment transport.

The submarine canyon "Swatch of No Ground" (SONG) cuts deeply into the inner shelf and is a major sediment trap and transport divide (Segall and Kuehl 1992; 1994; Kudrass et al. 1998), in which at least 10% of the total sediment load is temporarily deposited (Michels et al. 2000). Some of the sediment also may be transported directly onto the Bengal deep-sea fan (Kuehl et al.1989, Weber et al. 1997). A much greater sediment sink is the clinoform foreset[4] beds of the submarine delta at water depths of 15–80 m (Kuehl et al. 1997; Michels et al. 1998), where at least 20% of the total sediment load accumulates. They show evidence of cyclone or earthquake-induced destabilization of the sediments (Kuehl et al. 1997; Michels et al. 1998).

To obtain these values for the sediment balance sediment cores must be acquired to establish absolute chronologies. Coring is hampered by the fact that the sediments in the shallow water region are well-sorted silts and sands (Segall and Kuehl 1994) that piston and gravity corers cannot penetrate.

[1]Institute for Joint Geoscientific Research (GGA), S3: Geochronology and Isotope Hydrology, Stilleweg 2, Hannover, Germany. Corresponding author. Email: Axel.Suckow@gga-hannover.de.
[2]Institute of Geological & Nuclear Sciences (GNS), Lower Hutt, New Zealand
[3]Federal Institute for Geosciences and Natural Resources (BGR), Germany
[4]The idioms "foreset," "topset" and "bottomset" describe the sedimentological patterns at the submarine delta front. They are indicated in Figure 1 and characterized from the seismic record. For details see Michels et al. (1998).

RADIOCARBON, Vol 43, Nr 2B, 2001, p 917–927
Proceedings of the 17th International ^{14}C Conference, edited by I Carmi and E Boaretto

The sediments often do not contain carbonates (Segall and Kuehl 1992). Organic carbon, if present, consists of woody fragments of terrestrial origin that are certainly reworked (Segall and Kuehl 1994). The deposition rates are often so high that the cores do not contain sediments from before 1954, the time of the first global anthropogenic bomb fallout in the environment (Kuehl et al. 1989; Kudrass et al. 1998). Reworking by cyclones results in graded layers, for which grain-size effects inhibit the use of excess-radionuclide dating models (Michels et al. 1998). It is therefore desirable to obtain information from as many geochronological methods as possible to obtain constraints for the sedimentation rates.

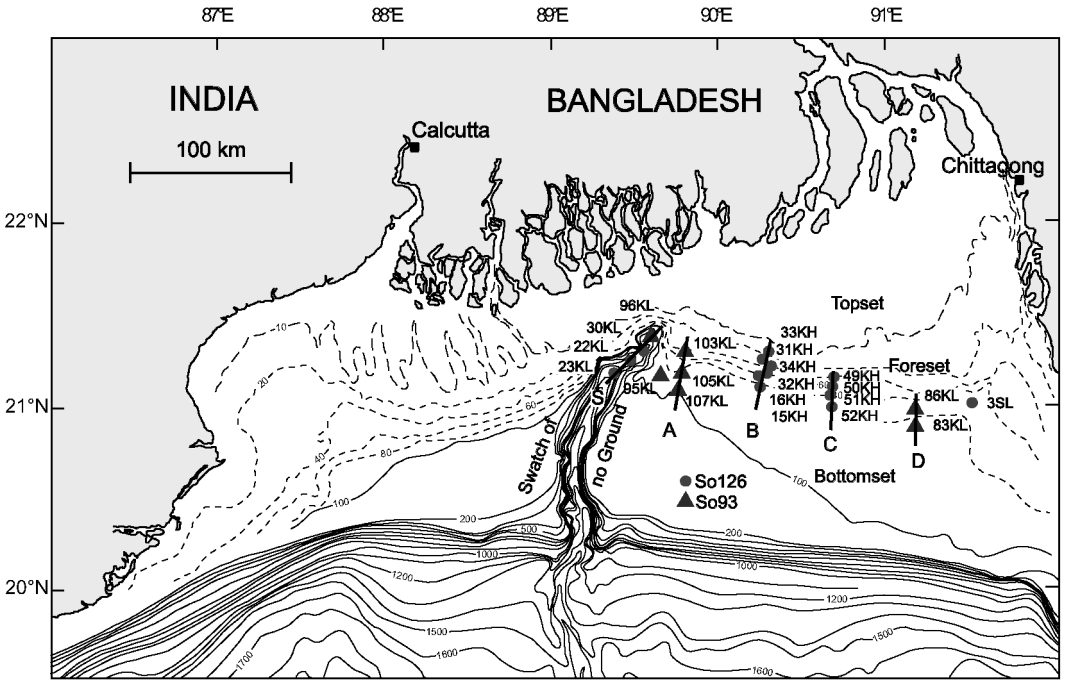

Figure 1 Bathymetric map of the study region showing the locations of the coring sites. KL= heavy piston corer, SL=gravity corer, KH= vibrocorer.

We combined the results of an extensive gamma spectrometric study (^{210}Pb, ^{137}Cs, ^{228}Ra) of more than twenty cores of young sediments and extended the chronology with ^{14}C ages for older carbonate-containing sediments and applied the ^{32}Si method to one core. Even though these geochronological results were consistent, the limited availability of cores and geochronological problems owing to sedimentation processes put severe constraints on the accuracy of the sediment balance.

METHODS

Core samples from the submarine delta and SONG were taken during two cruises with the research vessel "FS Sonne" in 1994 (So93) and 1998 (So126). Core positions are given in Figure 1. We used a vibrocorer (KH) for sandy sequences, obtaining cores up to 3.8 m long. In muddy sediments, a gravity corer (SL) and a heavy piston corer (KL) produced cores up to 17 m long.

Cores were cut in half lengthwise onboard after multi-sensor core logging. Most samples for gamma spectrometric dating were taken onboard from the centre of the sediment column, where disturbance

https://doi.org/10.1017/S0033822200041588 Published online by Cambridge University Press

due to the coring could be excluded. The samples were freeze dried, placed in PVC beakers to a defined height, diameter and weight, sealed air-tight, and stored for at least four weeks to attain radioactive equilibrium between ^{214}Pb and ^{226}Ra. A well-type detector with an active volume of 240 cc and an n-type detector of 25% relative efficiency was used for the gamma spectrometric measurements. Both detectors are specially designed for extra-low background. Spectra were taken using standard EG&G Ortec electronics (92X and 92X-II) and evaluated using GammaVision software. The efficiencies of the detectors were calibrated using the IAEA standard materials RgU-1, RgTh-1, and RgK-1, as well as standards prepared by adding the standard radionuclide solutions ML1 and ML4 (PTB) to sediments from core 105KL below 4 m depth and drying.

For data handling, LabData software was used (Suckow and Dumke 2001), which also routinely computes sediment ages using the constant flux (cf), constant initial concentration (cic) and constant sedimentation rate (csr) ^{210}Pb age dating models (Appleby and Oldfield 1992). Sedimentation rates resulting from the ^{137}Cs values were derived using the lowermost sample in which ^{137}Cs was detectable and assigning it an age of 40 years (So93) or 44 years (So126), corresponding to the beginning of ^{137}Cs fallout in 1954. An additional age estimate was derived from the gamma spectra on the basis of the deficiency of ^{228}Ra relative to ^{232}Th (Dukat and Kuehl 1995). Radium is leached from the sediments during transport in water. After deposition, the resulting radioactive deficiency decreases until secular equilibrium with the parent nuclides ^{230}Th and ^{232}Th is again attained. ^{226}Ra can be treated as stable since its half-life (1600 a) is long compared with the half-life of ^{228}Ra (5.75 a). When the ^{228}Ra/^{226}Ra activity ratio is used instead of ^{228}Ra, geochemical variations within the sediment pile are removed from the depth profile. The ^{228}Ra/^{226}Ra activity ratios measured by gamma spectrometry were plotted versus depth and compared with theoretical ingrowth curves.

From those parts of the cores for which gamma spectrometric data indicated sediments older than several centuries, several kilograms of sediment were sieved to extract sufficient carbonate material for radiocarbon dating. These samples were sent to Beta Analytic Inc. (Florida, USA) for AMS dating. To estimate the reservoir effect, two sediment-feeding worms that were found alive in core 21SL were dated using miniature counters in Hannover (Jelen and Geyh 1986).

To determine the ^{32}Si activity, the procedure for extraction of biogenic silica described by DeMaster (1980) was used. These samples were send to GNS in Lower Hutt, New Zealand, where the silica was purified, and the ^{32}Si activity measured by "milking" the daughter isotope ^{32}P. A low-background liquid scintillation counter (Quantulus 1220) was used. Details of the purification and measurement procedure are described by Morgenstern et al. (2001). Ages were calculated using a ^{32}Si half-life of 140 a (Morgenstern et al. 1996).

RESULTS

The results of gamma dating of samples from the cores taken along transects S, A, and D have been described by Michels et al. (1998, 2000) and Kudrass et al. (1998). All cores from transects B and C (Figure 1) at the middle of the main delta front contained measurable ^{137}Cs down to the bottom of the core. The two longest of these cores are 318 cm (52KH) and 380 cm (15KH). Concentrations of $^{210}Pb_{exc}$ and ^{137}Cs were found to be a function of grain size, as observed in earlier studies (Dukat and Kuehl 1995; Goodbred and Kuehl 1998; Michels et al. 1998). Core 33KH contained cross-stratified sands in the upper 50 cm and no detectable ^{137}Cs down to a depth of 135 cm. Below this depth, clay lumps within the sand contained detectable ^{137}Cs. Core 31KH was also cross-stratified, contained no ^{137}Cs down to a depth of 90 cm, but the four samples from below this depth had ^{137}Cs activities up

https://doi.org/10.1017/S0033822200041588 Published online by Cambridge University Press

to 3 Bq/kg (Figure 2). The other cores from these transects had measurable ^{137}Cs and $^{210}Pb_{exc}$ activities in nearly all samples (Figure 2).

For sediments below the layer containing ^{137}Cs, the mean value of the $^{228}Ra/^{226}Ra$ activity ratio for all cores was 1.8 with a standard deviation of ±0.1. In all cores containing ^{137}Cs-free sediments below a certain depth, these ratios increase with increasing depth. But the northern cores from transects B and C did not show measurable leaching of radium in the depth profile, and in these cores the $^{228}Ra/^{226}Ra$ activity ratio was less than 1.8 throughout the core (Figure 2).

A ^{32}Si sample from 475–515 cm depth in core 23KL had a specific activity of 4.9 ± 0.43 dpm/kg. On the basis of gamma dating, the age of this sediment layer is 39 years (Michels et al. 2000). Therefore, an initial ^{32}Si activity of 5.9 dpm/kg was calculated for this region, using decay correction. Specific ^{32}Si activities in samples from core 105KL decrease with increasing depth. Calculation of ^{32}Si ages is described by Morgenstern et al. (2001).

The sediment worms found in 21SL yielded a ^{14}C value of 101.8 ± 1.6 pMC and a $\delta^{13}C$ value of –19.7‰. The ^{14}C activity of carbonates from core 105KL did not decrease with depth, whereas in core 107KL they did.

DISCUSSION

Radionuclide inventories of ^{137}Cs and $^{210}Pb_{exc}$ showed a good linear correlation of inventory with sedimentation rate (Figure 3). This demonstrated that the ^{137}Cs and $^{210}Pb_{exc}$ was transported with the sediment and was not due to direct in-situ atmospheric deposition. In the latter case, the inventory would be constant for all sedimentation rates. So the sedimentation was focused at the depocenter of the delta front and the "Swatch of No Ground".

The absence of ^{137}Cs in the fine to medium-grained sand of the northern cores from transects B and C (Figure 1) was interpreted as a grain-size effect: coarser grained parts of a graded layer contain less ^{137}Cs than synsedimentary finer grained parts. This is observed in the sand layers in other cores (Michels et al. 1998). Even if the sediments contain no ^{137}Cs, they may be very young. This was indicated by the anthropogenic fallout detected in deeper sediments, which contain a higher percentage of clay. As all cores from transects B and C contained measurable ^{137}Cs down to the bottom of the core, and since the known pattern of atmospheric radionuclide deposition with respect to time was not discernible in the depth profiles, only minimum sedimentation rates can be derived from $^{210}Pb_{exc}$ and ^{137}Cs. In these cases, a sedimentation rate can be estimated from the $^{228}Ra/^{226}Ra$ activity ratio only (Dukat and Kuehl 1995). For at least two reasons, this estimate is not very precise:

1. The initial $^{230}Th/^{232}Th$ activity ratio might not have been constant, but varied with the coring site. For example, cores 30KL, 22KL, 23KL from "Swatch of No Ground" had $^{228}Ra/^{226}Ra$ activity ratios of 1.7, 1.7 and 1.8, respectively, in sediments below the interval containing ^{137}Cs. This ratio was 2 in core 95KL, taken just out this submarine canyon. While this difference was within two standard deviations of the mean of all sediments, it could also be due to a transport-related density sorting of mineral grains with different initial $^{238}U/^{232}Th$ ratios.
2. The amount of leached radium is unknown and not necessarily constant: Moore (1997) found the radium activities in shallow water in this region are higher than can be explained on the basis of sediment leaching and that these activities show seasonal variation depending on the monsoons. Thus, the amount of leached ^{228}Ra should also vary with the radium concentration in the water. Taking these two factors into account, we fitted the theoretical ingrowth curves for ^{228}Ra as well as possible to the depth profiles. The large spread between the minimum and maximum

https://doi.org/10.1017/S0033822200041588 Published online by Cambridge University Press

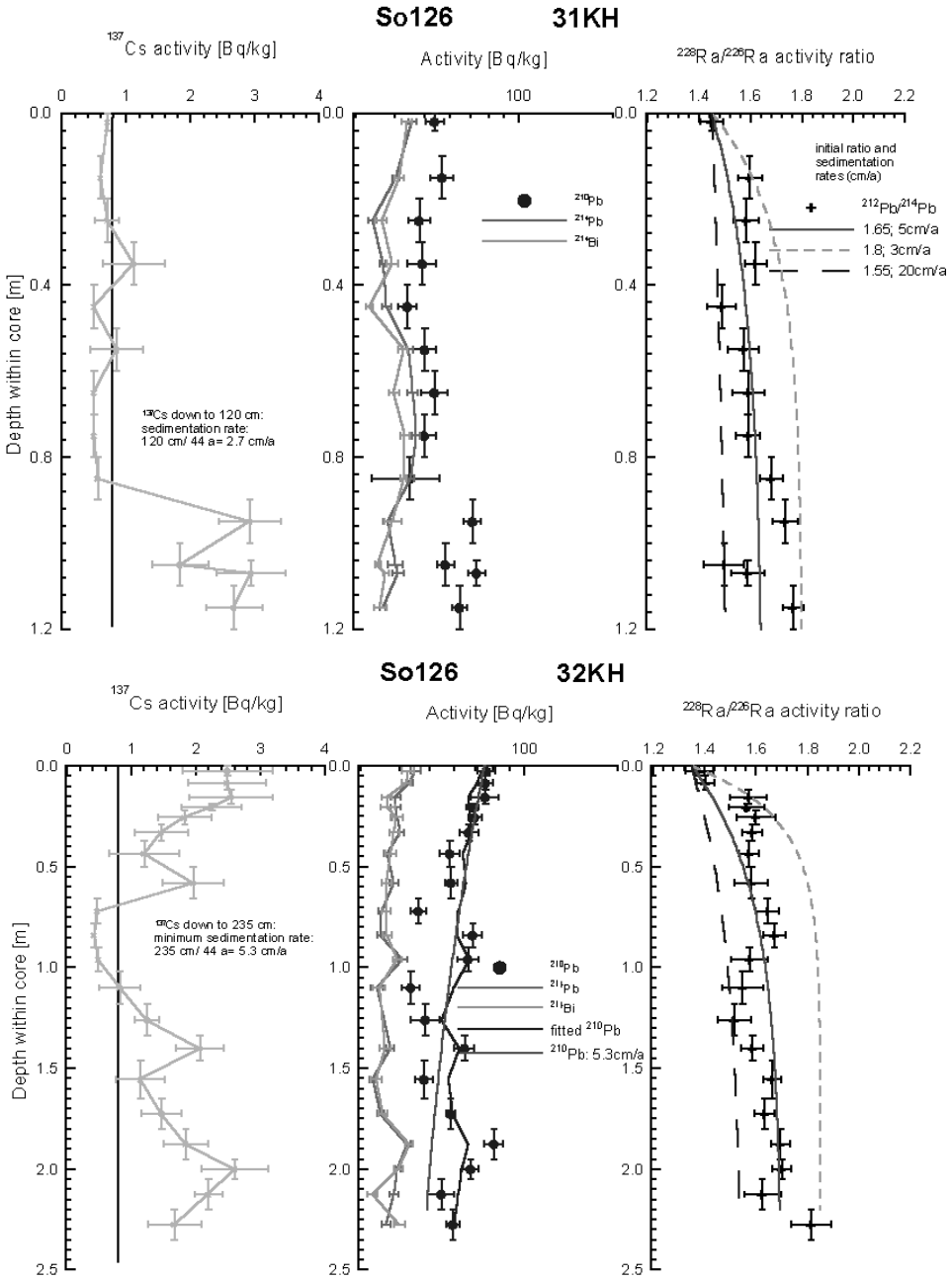

Figure 2 Depth profiles for the radionuclides measured by gamma spectrometry for cores 31KH (a), 32KH (b), 52KH (c), 95KL (d) as examples for cores from the foreset beds. ^{226}Ra is measured as activity of the daughter ^{214}Pb (352keV) and ^{228}Ra as activity of the daughter ^{212}Pb (238.6keV), where both mother-daughter pairs can be assumed to be in secular equilibrium.

https://doi.org/10.1017/S0033822200041588 Published online by Cambridge University Press

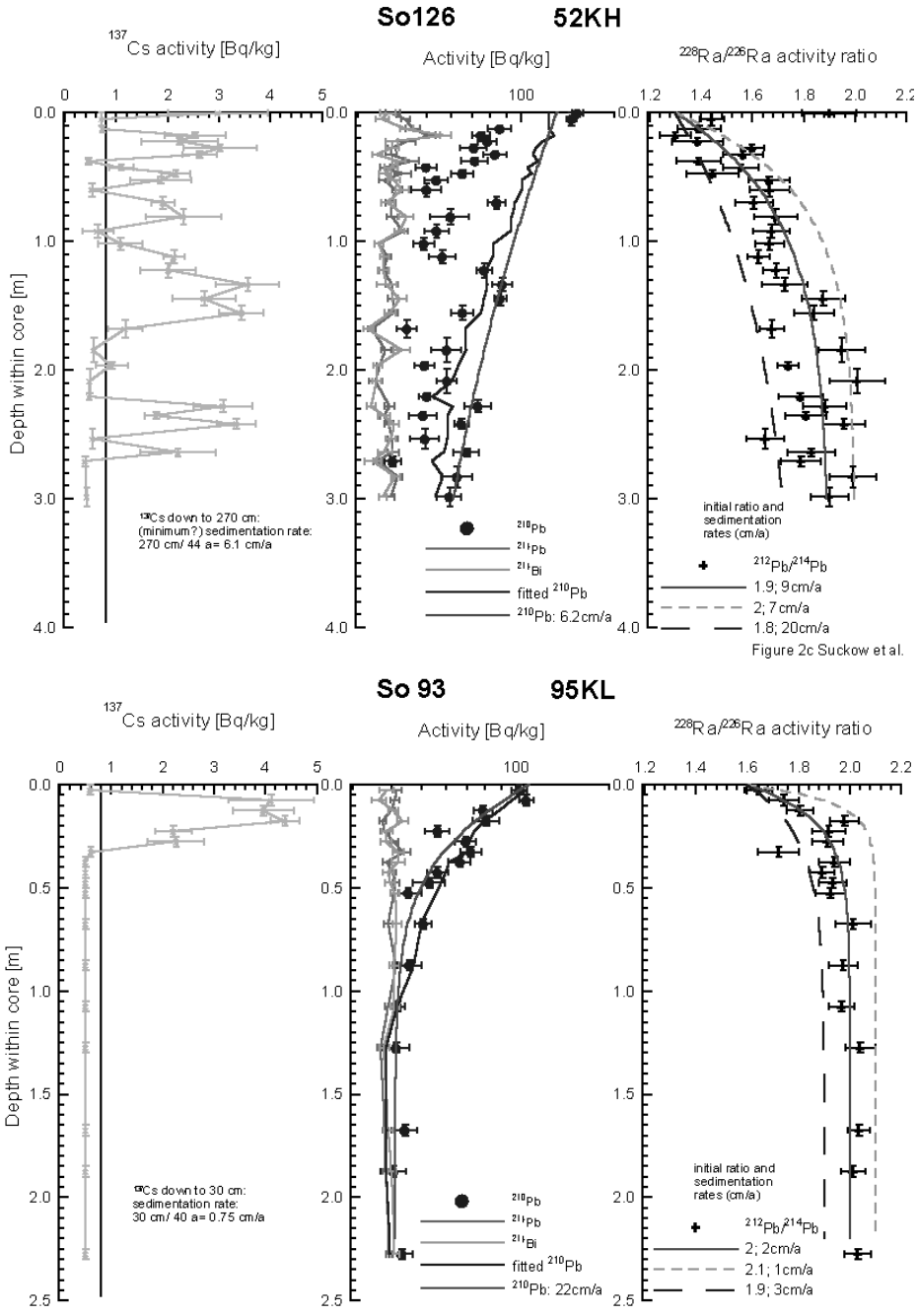

Figure 2 (*Continued*) Depth profiles for the radionuclides measured by gamma spectrometry for cores 31KH (a), 32KH (b), 52KH (c), 95KL (d) as examples for cores from the foreset beds. ^{226}Ra is measured as activity of the daughter ^{214}Pb (352keV) and ^{228}Ra as activity of the daughter ^{212}Pb (238.6keV), where both mother-daughter pairs can be assumed to be in secular equilibrium.

https://doi.org/10.1017/S0033822200041588 Published online by Cambridge University Press

sedimentation rates was mainly due to the different initial ratios derived from the standard deviation (±0.1; Figure 2) of the mean $^{228}Ra/^{226}Ra$ activity ratio of all sediments. The resulting estimate certainly cannot be treated as more than a reasonable guess. But since all of the other geochronological methods failed for transects B and C, these estimates are the best available for the sedimentation rates.

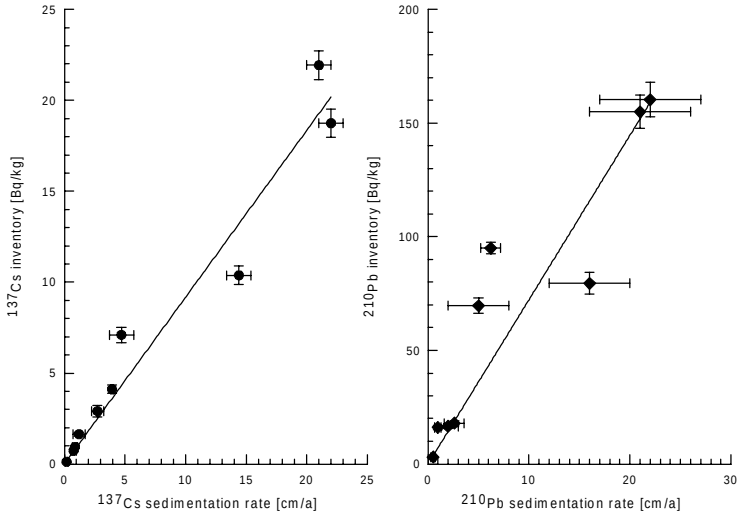

Figure 3 Linear dependence between the radionuclide inventory of ^{137}Cs and $^{210}Pb_{exc}$ and the sedimentation rate. Only cores containing the lower boundary of ^{137}Cs-bearing sediments are included.

A general problem for the interpretation of the radionuclide depth profiles for the sandy topset beds was that they could indicate a sedimentation rate (assuming final deposition, i.e., deposition without subsequent reworking) or the depth of maximum recent reworking (assuming dynamic equilibrium between sediment transport to the core position and away from it). Wave energy during tropical storms is probably high enough to rework sandy sediments down to a depth of 30 m (Barua and Kana 1995; Booth and Winters 1991). On the basis of ^{137}Cs alone, no decision was possible, since the sediments could have been reworked by a storm several weeks before the coring, so that grain-size effects could have produced the measured pattern of radionuclides. The ^{228}Ra leaching indicated by lower $^{228}Ra/^{226}Ra$ activity at the seafloor than below, it pointed to an increasing age of the sediment with depth. In these cases, final sediment deposition several years ago was more plausible. But processes on a larger time scale (several decades) could, however, rework the sediment again. Other cores from water depths greater than 30 m consisted of multi-layered clay-silt-sand sequences, each representing a single major transport and deposition event. Also in these cases, final deposition was more probable. So while continuous reworking and final deposition cannot be distinguished in general, final deposition becomes more probable with increasing water depth, and for some cores evidence as described indicated final deposition. For the cores 33KH, 32KH and 49KH a decision was not possible and for the sediment balance computations they were, therefore, not taken into consideration.

Assuming final deposition, we took the sedimentation rates given in Table 1 as a preliminary estimate and calculated the volume of sediment deposited annually using the kriging procedure of the

https://doi.org/10.1017/S0033822200041588 Published online by Cambridge University Press

Surfer® software. Based on the sedimentation rates for all cores from the foreset beds (Figure 1) estimated from ^{137}Cs activity, this resulted in a minimum annual sediment volume of 2.4×10^8 m^3 deposited in the foreset beds. Application of the same procedure using the values derived from the ^{228}Ra/^{226}Ra activity ratio instead of the minimum values for sedimentation rates from ^{137}Cs yielded a sediment volume of 3.1×10^8 m^3. With the numbers given in the introduction, these volumes correspond to 24% and 31%, respectively, of the annual sediment load of the Ganges-Brahmaputra river system. Varying the parameter values for the numerical interpolation process (e.g. for the kriging parameters, like anisotropy, angle of the main axis of the search ellipse) resulted in only 10% variation around these values.

Table 1 Locations, radionuclide inventories, and sedimentation rates of the sediment cores dated by gamma spectrometry

Core	East	North	^{210}Pb inventory (Bq/m^2)	csr-sedimentation rate (cm/a)	^{137}Cs inventory (Bq/m^2)	Mean ^{137}Cs sedimentation rate (cm/a)	^{228}Ra estimate for sedimentation rate (cm/a)	
							Best estimate	Range
96KL	89.577	21.350	128.4	n.d.	41.2	>28	50	30–70
30KL	89.564	21.307	154.9	21.0	21.9	22.8	22	18–25
22KL	89.485	21.252	160.3	22.0	18.7	20.7	20	18–25
23KL	89.390	21.186	79.5	16.0	10.4	12.4	13	10–20
95KL	89.665	21.167	16.1	1.0	0.7	0.8	2	1–3
103KL	89.800	21.299	8.5	n.d.	2.9	2.7	5	2–10
105KL	89.783	21.189	17.9	2.6	1.6	1.2	2	1–5
107KL	89.767	21.110	3.0	0.5	0.1	0.2	1	0.2–2
33KH	90.247	21.264	0.2	n.d.	0.1	>3.2	n.d.	n.d.
31KH	90.229	21.202	14.1	n.d.	0.8	>2.8	5	3–20
34KH	90.237	21.191	19.9	n.d.	0.9	>5.1	7	4–10
32KH	90.219	21.163	58.3	n.d.	3.3	>5.5	7	3–10
16KH	90.214	21.145	80.2	n.d.	6.2	>7.2	10	6–15
15KH	90.203	21.106	44.5	n.d.	3.7	>4.7	7	4–10
50KH	90.666	21.104	21.3	n.d.	0.0	>6	6	3–10
51KH	90.658	21.073	85.1	n.d.	8.2	>6.7	20	5–50
52KH	90.667	21.012	77.9	n.d.	4.1	>6.3	9	7–20
86KL	91.154	20.989	69.7	5.0	7.1	4.7	5	2–20
83KL	91.156	20.918	16.6	2.0	0.9	0.9	n.d.	n.d.
3SL	91.492	21.030	95.0	6.2	4.1	3.9	4	2–10

^{14}C ages were determined for samples from two cores containing older sediment (105KL and 107KL). Since the reservoir effect in this region is not known, it was estimated to be between 530 and 610 a on the basis of the measured activity (102 pMC) in the worms found in 21SL and the 110–109 pMC of the atmosphere in 1996 and 1997 (Doug Harkness, personal communication). One has to assume that the reservoir effect has a seasonal cyclicity owing to variations in the discharge from the Ganges Brahmaputra river system. Therefore, we used a value of 600 a, but believed that it cannot be better constrained than to one or two centuries. An additional, and probably more severe problem concerning the ^{14}C ages resulted from the fact that the carbonates (sand dollars and mollusc shells) were most probably not formed in situ, but reworked and then redeposited in the foreset beds.

Ages for core 105KL derived from gamma spectrometric dating using $^{210}Pb_{exc}$ and ^{137}Cs are compared in Figure 4 (left) with ^{32}Si-derived sediment ages and ^{14}C ages determined using a reservoir effect of 600 yr. The correlation of the age estimates derived for the different time scales was much

https://doi.org/10.1017/S0033822200041588 Published online by Cambridge University Press

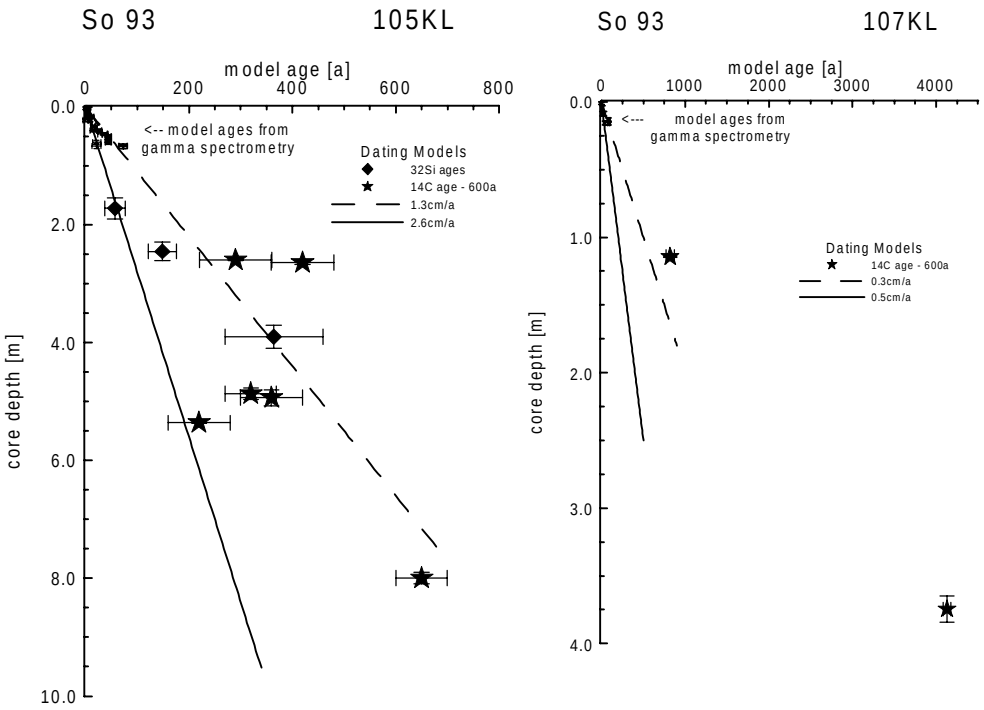

Figure 4 Comparison of ages derived from gamma spectrometry, ^{32}Si and ^{14}C for cores 105KL (left) and 107KL (right). A 600 yr reservoir effect has been applied to the ^{14}C ages. The thick solid and dashed lines are sediment ages calculated assuming a constant sedimentation rate of 2.6 and 1.3 cm/a, respectively. A fourth ^{32}Si sample from a core depth of 6.0 m yielded an age at the detection limit of the method.

better than expected. Our interpretation was that the sediment chronology resulting from gamma spectrometry can be extrapolated reasonably over several centuries if one keeps in mind that the sedimentation rate cannot be estimated with a precision of better than 50%. The other dating methods faced similar problems and cannot be considered to be more precise. On the other hand, the sedimentation rate cannot be extrapolated to millennia (Figure 4, right): 107KL shows lower sedimentation rates on a time scale of several millennia derived from ^{14}C. This was understandable when sedimentation at the delta front is taken into account. The lowest sedimentation rate at a specific position should be when this position is in the bottomset area of the delta front. Sedimentation rates peak in the foreset beds, and there is probably no net sedimentation in the topset beds—only reworking of the sediment. Therefore, we expected lower sedimentation rates for older sediments when the core position at that time was seawards of the foreset beds.

CONCLUSIONS

Geochronological work in the Bengal shelf area was hampered by storm-induced sediment reworking, grain-size effects, problems to obtain cores long enough to establish a chronology longer than a century, scarcity of carbonates, and an unknown ^{14}C reservoir effect. Nevertheless, a gamma spectrometric survey using the nuclides ^{137}Cs, ^{210}Pb and ^{228}Ra resulted in an estimated sediment volume of 2.4–3.1×10^{8} m^{3} deposited annually in the foreset beds, corresponding to 24–31% of the total annual sediment load of the Ganges-Brahmaputra river system. Comparison of ages derived from gamma spectrometry with those from ^{32}Si and ^{14}C indicated the gamma data are reliable within the respective

https://doi.org/10.1017/S0033822200041588 Published online by Cambridge University Press

error and can probably be extrapolated up to a time scale of a few centuries. As the depocenter moves southward, different sedimentation rates were obtained when the sedimentation rates obtained for a time scale of decades (gamma spectrometry) were compared with those obtained for a time scale of millennia (^{14}C). Hence, a long-term sediment balance based on ^{14}C ages would probably be more reliable than one based on gamma spectrometry, but is hampered by the problems encountered in the attempt to obtain cores with a length of several tens of meters from the submarine delta. On the other hand, sedimentation processes, like storm-induced reworking, or grains-size effects in graded layers, are better studied and understood on the short time scale of decades using gamma spectrometry. In any case, an environment like the Bengal shelf in which complex processes take place requires as many geochronological approaches as possible to obtain a reliable chronology.

ACKNOWLEDGMENTS

The authors wish to express their thanks to Gudrun Drewes, Sabine Mogwitz, Petra Posimowski, and Martina Schmidtke for processing the samples for gamma analysis. Werner Gräsle provided helpful information about Surfer interpolation routines.

REFERENCES

Allison MA. 1998. Historical changes in the Ganges-Brahmaputra delta front. *Journal of Coastal Research* 14:480–90.

Allison MA, Kuehl SA, Martin TC, Hassan A. 1998. Importance of floodplain sedimentation for river sediment budgets and terrigeneous input to the oceans: insights for the Brahmaputra-Jamuna river. *Geology* 26: 175–8.

Appleby PG, Oldfield F. 1992. Application of lead-210 to sedimentation studies. In: Ivanovich M, Harmon RS, editors. *Uranium series disequilibrium. Applications to Earth, marine and environmental sciences*. Oxford: Clarendon Press. p 731–79.

Barua DK, Kuehl SA, Miller RL, Moore WS. 1979. Suspended sediment distribution and residual transport in the coastal ocean off the Ganges-Brahmaputra river mouth. *Marine Geology* 120:41–61.

Barua DK, Kana TW. 1995. Deep water wave hindcasting, wave refraction modelling and wind and wave induced motions in the east Ganges-Brahmaputra delta coast. *Journal of Coastal Research* 11(3):834–48.

Booth JS, Winters WJ. 1991. Wave processes and geologic responses on the floor of the Yellow Sea. In: *From shoreline to abyss.* Society for Sedimentary Geology. Special publication. p 123–32.

DeMaster DJ. 1980. The half-life of ^{32}Si determined from a varved Gulf of California sediment core. *Earth and Planetary Science Letters* 48:209–17.

Dukat DA, Kuehl SA. 1995. Non-steady-state ^{210}Pb flux and the use of $^{228}Ra/^{226}Ra$ as a geochronometer on the Amazon continental shelf. *Marine Geology* 125:329–50.

Goodbred SL, Kuehl SA. 1998. Floodplain processes in the Bengal Basin and the storage of Ganges-Brahmaputra river sediment: an accretion study using ^{137}Cs and ^{210}Pb geochronology. *Sedimentary Geology* 21: 239–58.

Goodbred SL, Kuehl SA. 1999. Holocene and modern sediment budgets for Ganges-Brahmaputra river: evidence for highstand dispersal to floodplain, shelf and deep-sea depocenters. *Geology* 27: 559–62.

Jelen K, Geyh MA. 1986. A low-cost miniature counter system for radiocarbon dating. *Radiocarbon* 28(2A): 578–85.

Kudrass HR, Michels KH, Wiedicke M, Suckow A. 1998. Cyclones and tides as feeders of a submarine canyon off Bangladesh. *Geology* 26:715–18.

Kuehl SA, Hariu TM, Moore WS. 1989. Shelf sedimentation off the Ganges-Brahmaputra river system: evidence for sediment bypassing to the Bengal fan. *Geology* 17:1132–5.

Kuehl SA, Levy BM, Moore WS, Allison MA. 1997. Subaqueous delta of the Ganges-Brahmaputra river system. *Marine Geology* 144:81–96.

Michels KH, Kudrass HR, Hübscher C, Suckow A, Wiedicke M. 1998. The submarine delta of the Ganges-Brahmaputra: cyclone-dominated sedimentation patterns. *Marine Geology* 149:133–54.

Michels K, Suckow A, Breitzke M, Kudrass HR, Kottke B. 2001. The role of a shelf canyon as a temporary depocenter between river mouth and deep-sea fan. *Deep-Sea Research.* Forthcoming.

Milliman JD, Meade RH. 1983. World-wide delivery of river sediment to the oceans. *Journal of Geology* 91:1–21.

Moore WS. 1997. High fluxes of radium and barium from the mouth of the Ganges-Brahmaputra river during low river discharge suggest a large groundwater source. *Earth and Planetary Science Letters* 150:141–50.

Morgenstern U, Taylor CB, Parrat Y, Gäggeler HW, Eichler B. 1996. ^{32}Si in precipitation: evaluation of

temporal and spatial variation and as dating tool for glacial ice. *Earth and Planetary Science Letters* 144: 289–96.

Morgenstern U, Geyh MA, Kudrass HR, Ditchburn RG, Graham IJ. 2001. ^{32}Si dating of marine sediments: application to the shelf of Bangladesh. *Radiocarbon.* This issue.

Segall MP, Kuehl SA. 1992. Sedimentary processes on the Bengal shelf as revealed by clay-size mineralogy. *Continental Shelf Research* 12:517–41.

Segall MP, Kuehl SA. 1994. Sedimentary structures on the Bengal shelf: a multi-scale approach to sedimentary fabric interpretation. *Sedimentary Geology* 93: 165–80.

Suckow A, Dumke I. 2001. A database system for geochemical, isotope hydrological and geochronological laboratories. *Radiocarbon.* This issue.

Weber ME, Wiedicke MH, Kudrass HR, Hübscher C, Erlenkeuser H. 1997. Active growth of the Bengal Fan during sea-level rise and highstand. *Geology* 25:315–18.